ADVANCED HEALTHCARE MATERIALS
www.advhealthmat.de

Spatiotemporally Controlled Release of Rho-Inhibiting C3 Toxin from a Protein–DNA Hybrid Hydrogel for Targeted Inhibition of Osteoclast Formation and Activity

Jasmina Gačanin, Anna Kovtun, Stephan Fischer, Victoria Schwager, Johanna Quambusch, Seah Ling Kuan, Weina Liu, Felix Boldt, Chuang Li, Zhongqiang Yang, Dongsheng Liu, Yuzhou Wu, Tanja Weil, Holger Barth,* and Anita Ignatius**

In osteoporosis, bone structure can be improved by the introduction of therapeutic molecules inhibiting bone resorption by osteoclasts. Here, biocompatible hydrogels represent an excellent option for the delivery of pharmacologically active molecules to the bone tissue because of their biodegradability, injectability, and manifold functionalization capacity. The present study reports the preparation of a multifunctional hybrid hydrogel from chemically modified human serum albumin and rationally designed DNA building blocks. The hybrid hydrogel combines advantageous characteristics, including rapid gelation through DNA hybridization under physiological conditions and a self-healing and injectable nature with the possibility of specific loading and spatiotemporally controlled release of active proteins, making it an advanced biomaterial for the local treatment of bone diseases, for example, osteoporosis. The hydrogels are loaded with a recombinant Rho-inhibiting C3 toxin, C2IN-C3lim-G205C. This toxin selectively targets osteoclasts and inhibits Rho-signaling and, thereby, actin-dependent processes in these cells. Application of C2IN-C3lim-G205C toxin-loaded hydrogels effectively reduces osteoclast formation and resorption activity in vitro, as demonstrated by tartrate-resistant acid phosphatase staining and the pit resorption assay. Simultaneously, osteoblast activity, viability, and proliferation are unaffected, thus making C2IN-C3lim-G205C toxin-loaded hybrid hydrogels an attractive pharmacological system for spatial and selective modulation of osteoclast functions to reduce bone resorption.

1. Introduction

Bone turnover is an active process resulting from the well-orchestrated interplay between bone-forming cells (osteoblasts) and bone-resorbing cells (osteoclasts). Their cross-talk is tightly regulated by hormones, including parathormone,[1,2] cytokines, for example, interleukin 6,[3] and growth factors, including bone morphogenetic proteins (BMPs) 2 and 7.[1] Disequilibrium in this complex interplay leads to an imbalance between bone formation and resorption, which results in severe bone diseases, including osteoporosis, and affects regeneration processes after both injuries and surgical intervention.[4,5] Therefore, optimizing skeletal repair in the context of osteoporosis is an important scientific and medical aim. Bone structure improvement can be achieved by enhancing bone formation with therapeutic molecules, including BMPs,[6,7] and repressing resorption using, for example, bisphosphonates.[7–9] To achieve local delivery of therapeutically active compounds in bone defects or

J. Gačanin, J. Quambusch, W. Liu, F. Boldt, Prof. Y. Wu, Prof. T. Weil
Institute of Organic Chemistry III
University of Ulm
89081 Ulm, Germany
E-mail: wuyuzhou@hust.edu.cn

Dr. A. Kovtun, Prof. A. Ignatius
Institute of Orthopedic Research and Biomechanics
Trauma Research Center
University of Ulm
89081 Ulm, Germany
E-mail: anita.ignatius@uni-ulm.de

S. Fischer, V. Schwager, Prof. H. Barth
Institute of Pharmacology and Toxicology
University of Ulm
89081 Ulm, Germany
E-mail: holger.barth@uni-ulm.de

J. Quambusch, Dr. S. L. Kuan, Prof. Y. Wu, Prof. T. Weil
Max Planck Institute for Polymer Research
55128 Mainz, Germany

Dr. C. Li, Prof. Z. Yang, Prof. D. Liu
Key Laboratory of Organic Optoelectronics and Molecular Engineering of the Ministry of Education
Department of Chemistry
Tsinghua University
100084 Beijing, China

Prof. Y. Wu
School of Chemistry and Chemical Engineering
Huazhong University of Science and Technology
430074 Wuhan, China

DOI: 10.1002/adhm.201700392

weak bone, for example, immediately surrounding implants, an appropriate carrier is crucial to achieve sustained in situ release of therapeutic molecules. Here, biocompatible hydrogels could represent one of the best options for achieving an efficient local delivery system. The high water content imparts biocompatibility and a large number of therapeutics could be loaded and delivered via a controllable slow-release mechanism.[10]

It has been shown previously that the delivery of therapeutic molecules into bone tissue is possible via absorption of the therapeutic within a synthetic hydrogel,[11] physically crosslinked alginate-gel[12] or Matrigel[13] during hydrogel preparation. Recently, we developed a biodegradable and biocompatible protein–DNA hybrid hydrogel, which is crosslinked by DNA hybridization without the application of reactive organic reagents or catalysts. DNA hybridization is based on sequence-specific, supramolecular interactions, providing the hydrogel with beneficial features, including being injectable and self-healing.[14] Importantly, it is this injectable nature, which allows for simple, local administration of the protein–DNA hybrid hydrogel via injection at the diseased site. In contrast to the incorporation of guest molecules via absorption, protein–DNA hydrogels offer the opportunity to readily assemble the desired bioactive molecules within the hydrogel using the appropriately functionalized DNA adaptors. Even different kinds of functional proteins could be immobilized successfully following this approach.[14] In this fashion, a highly controlled protein loading in combination with local release of the bioactive molecules could be achieved at the diseased site by nuclease-mediated cargo release. In contrast to conventional hydrogel scaffolds based on synthetic polymers or undefined mixtures, including Matrigel, with high batch-to-batch variations,[15] the protein–DNA hydrogels described herein feature a precisely defined composition and highly reproducible synthesis. Moreover, protein–DNA hybrid hydrogels provide several advantageous features, including adaptable polypeptide chain lengths, precisely defined amino acid sequences, and high biocompatibility.[16] In addition, further chemical modifications are facilitated by the presence of different functional groups along the main chain of the polypeptide backbone. The same strategy that converts proteins into versatile biomaterials combining biocompatibility, biodegradability, and multifunctionality has been studied previously in vitro and in vivo, demonstrating great potential for drug delivery[17,18] and bioimaging.[17,19,20] Therefore, this modular approach for the precise assembly of multicomponent and biodegradable hydrogels based on supramolecular interactions of the DNA building blocks allows for the controlled assembly of various pharmacologically active proteins and enzymes within the hydrogel without the need for applying reactive or potentially toxic reagents. Moreover, spatiotemporally controlled cargo release from the hybrid hydrogel is achieved by DNase application, which allows protein-cargo release while maintaining their pharmacological activity. In addition to being extensively studied for systemic application during cancer treatment,[21] DNases have been reported to be well tolerated in patients with cystic fibrosis[22] and nephritis lupus.[23] In particular, bovine pancreatic DNase has been reported to not cause any evidence of systemic toxicity when applied by intravenous injections or by other parenteral routes, including intrathecal.[24] Therefore, DNase administration provides a simple and smart, yet biocompatible possibility for well-directed cargo release. To address the excessive bone resorption by osteoclasts in osteoporosis, the targeted pharmacological modulation of osteogenesis or osteoclast activity represents a favorable strategy. The clostridial Rho-inhibiting C3 toxins could be attractive candidates for this purpose, because the treatment of cultured osteoclast-like cells with these enzymes effectively decreased both osteoclast formation from monocytic progenitor cells and their resorption activity in vitro.[25] The C3 toxins (≈25 kDa) mono-ADP-ribosylate Rho in the cytosol inhibits Rho-mediated signal-transduction and results in reorganization of the actin cytoskeleton accompanied by a dramatic change in cell morphology and inhibition of central actin-associated cellular functions.[26,27] Moreover, C3 toxins, such as C3bot from *Clostridium (C.) botulinum*[28] and C3lim from *C. limosum*,[29] are efficiently taken up into the cytosol of cells of the monocyte/macrophage-line by an endocytic mechanism but not into the cytosol of other cell types, including epithelial cells and fibroblasts.[26] The recombinant fusion toxin C2IN-C3lim contains C3lim and the nontoxic C2IN portion of the *C. botulinum* C2 toxin,[26] which likely enhances the selective uptake of C2IN-C3lim into the cytosol of monocytes/macrophages and osteoclasts, because both cell populations are derived from the same lineage.[25] In these earlier studies, we identified C2IN-C3lim as the most efficient Rho-inhibitor for RAW 264.7 macrophages among the clostridial C3 enzymes. Additionally, we demonstrated that this fusion toxin ADP-ribosylates Rho in RAW 264.7 cells results in reorganization of F-actin, as demonstrated by DAPI/phalloidin-staining of C2IN-C3lim-treated cells, and finally in the characteristic changes of cell morphology.[25] We believe that incorporating C2IN-C3lim enzyme into the biocompatible protein–DNA hybrid hydrogel opens a new avenue for efficient and cell type-selective treatment of increased bone resorption, featuring local application of therapeutics, ensuring a high local concentration and spatiocontrolled cargo release (**Figure 1**).

Herein, we demonstrate the unique potential of this novel protein–DNA hybrid hydrogel for local application and controlled release of C2IN-C3lim for the targeted pharmacological inhibition of osteoclast formation and resorption activity without affecting osteoblasts.

2. Results and Discussion

2.1. Preparation of C2IN-C3lim-G205C

The fusion protein C2IN-C3lim (≈50 kDa) combining both the enzymatically inactive N-terminal region of the C2I-toxin C2IN (≈25 kDa) from *C. botulinum* and the enzymatically active toxin, C3lim, from *C. limosum* could efficiently and specifically inhibit osteoclast differentiation and growth as discussed previously.[25] To load C2IN-C3lim into the hydrogel, a cysteine mutant of this fusion protein was created. As described in the experimental design, we replaced glycine at position 205 with cysteine to create the C2IN-C3lim-G205C mutant, suitable for accomplishing thiol-based bioconjugation reactions. Gly-205 was selected, because it is located on the surface of the folded protein and, therefore, the mutation is accessible for DNA conjugation. After expression as the glutathione S-transferase (GST)-fusion

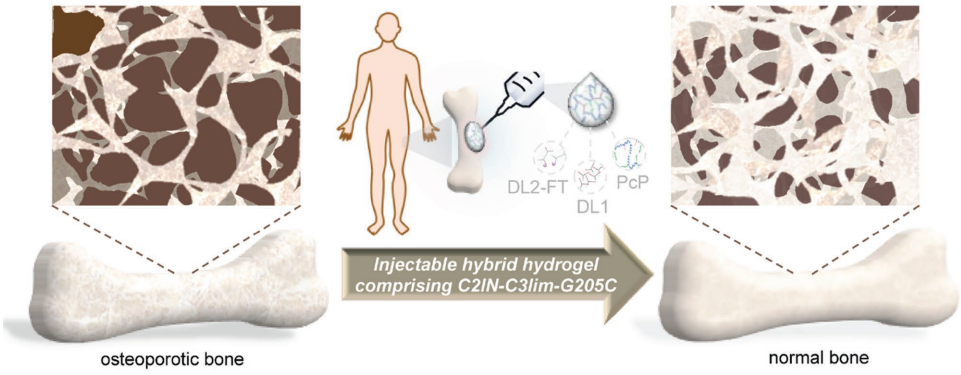

Figure 1. Design concept – inhibition of local bone resorption via administration of injectable protein–DNA hybrid hydrogel featuring spatiotemporally controlled release of Rho-inhibiting C3 toxin. Inhibition of bone resorption can be realized by the selective targeting of the formation and activity of osteoclasts, allowing for efficient bone regeneration (DL2-FT: C2IN-C3lim-G205C toxin-loaded DL2 DNA linker, DL1: DNA linker for crosslinking, PcP: protein-derived polypeptide copolymer backbone of the hydrogel).

protein in *Escherichia coli* and purification by affinity chromatography using the glutathione-sepharose system, the identity and complete expression of the toxin was confirmed by sodium dodecyl sulfate-polyacrylamide gel electrophoresis (SDS-PAGE) and subsequent western blotting using specific antibodies. According to Coomassie blue staining (**Figure 2**A) and antibody staining, both the C2IN and C3 regions could be detected at the expected height by specific antitoxin antibodies (Figure 2B). The enzymatic activity of C2IN-C3lim-G205C was confirmed by ADP-ribosylation (Figure 2C). This ADP-ribosylation assay is well-established and represents the gold standard because of the very sensitive and specific detection of the modification of Rho by C3 toxins in cells.[25–30]

To confirm C2IN-C3lim-G205C uptake into the cytosol of living cells, J774A.1 macrophages were intoxicated with different amounts of C2IN-C3lim-G205C. Incubation of J774A.1 cells for 8 h with the newly generated C2IN-C3lim-G205C or the original C2IN-C3lim as a control, led to clear C3-induced morphological cell changes (Figure 2D). To demonstrate the toxins could ADP-ribosylate Rho, the cells were lysed and in vitro ADP-ribosylation was performed. The lysates were incubated with biotin-NAD$^+$ and fresh C2IN-C3lim-toxin. Rho in untreated cells was strongly ADP-ribosylated during the in vitro reaction, resulting in a strong signal in the western blot (Figure 2E). In contrast, less ADP-ribosylated Rho was detected when the macrophages were treated with C2IN-C3lim-G205C, indicating that Rho was already ADP-ribosylated in living cells during the incubation period. This assay (Figure 2E) clearly displayed a concentration-dependent intoxication. Loading of comparable amounts of total protein was confirmed by actin staining with specific antibodies. In summary, the results indicate the specific uptake of C2IN-C3lim-G205C into the cytosol of J774A.1 cells, whereas other cell types, including fibroblasts and epithelial cells, remained unaffected (data not shown).

2.2. Preparation of Toxin-Loaded Hydrogel

The synthesis of the hydrogel is based on a protocol reported previously. Briefly, human serum albumin (HSA) is first converted to cHSA (**Figure 3**A).[31] Thereafter, about 18 poly(ethylene glycol) (PEG) chains (M_w = 2000) are conjugated to the amino groups of cHSA to afford cHSA-PEG(2000)$_{18}$. Noteworthy, primary amino groups can originate from the newly introduced amino groups of the previous synthetic step as well as from lysine side chains of cHSA. For clarity reasons, the conjugation reaction in the scheme is only shown for the newly introduced amines and not for the lysine side chains. Residual amines are converted to azido groups by applying the diazo transfer reagent imidazole-1-sulfonyl azide hydrochloride yielding N$_3$-cHSA-PEG(2000)$_{18}$. The alkyne functionalized ssDNA sequence (alkyne-SE1′) is then conjugated to N$_3$-cHSA-PEG(2000)$_{18}$ via Huisgen cycloaddition yielding cHSA-PEG(2000)$_{18}$-SE1′$_8$ with on average eight SE1′ per polymer chain. Finally, cHSA-PEG(2000)$_{18}$-SE1′$_8$ is denatured in concentrated urea buffer, followed by reduction of the disulfide bridges by tris(2-carboxyethyl)phosphine (TCEP) and capping of the free sulfurhydryl groups as reported.[14] The stable and well soluble polypeptide copolymer dcHSA-PEG$_{18}$-SE1′$_8$ (PcP) is thus obtained, carrying PEG chains contributing water-solubility and ssDNA (SE1′) allowing the precise interaction with DNA crosslinkers as well as further functionalization.

The hydrogel was prepared from the PcP as depicted in Figure 3A, according to the previously reported protocol.[14] The detailed synthesis and characterization of all synthesis steps are summarized in Scheme S1 and Figures S3–S19 (Supporting Information). Gelation of the hydrogel is based on the crosslinking of the PcP with multiarm DNA crosslinker (DL1 and DL2 DNA linkers, **Figures** 3B and 4). DL2 allows loading of up to two C2INC3lim-G205C to its sticky ends SE3′ and SE4′, while DL1 serves as a small crosslinker to increase the crosslinking degree. Maleimide-modified DNA tag SE3′ was specifically conjugated to the single mutated cysteine residue of C2IN-C3lim-G205C (Figure 4). The conjugation of the SE3′ DNA tag to C2IN-C3lim-G205C did not influence the uptake of this toxin into macrophages or its ADP-ribosyltransferase activity in the cytosol of these cells (Figures S1 and S2, Supporting Information). Moreover, the coupling of the DNA tag to C2IN-C3lim-G205C had no effect on the viability of J774A.1 macrophages or RAW 264.7 monocytic cells, because the number of viable cells after 72 h was comparable when treated with C2IN-C3lim, C2IN-C3lim-G205C, or C2IN-C3lim-G205C

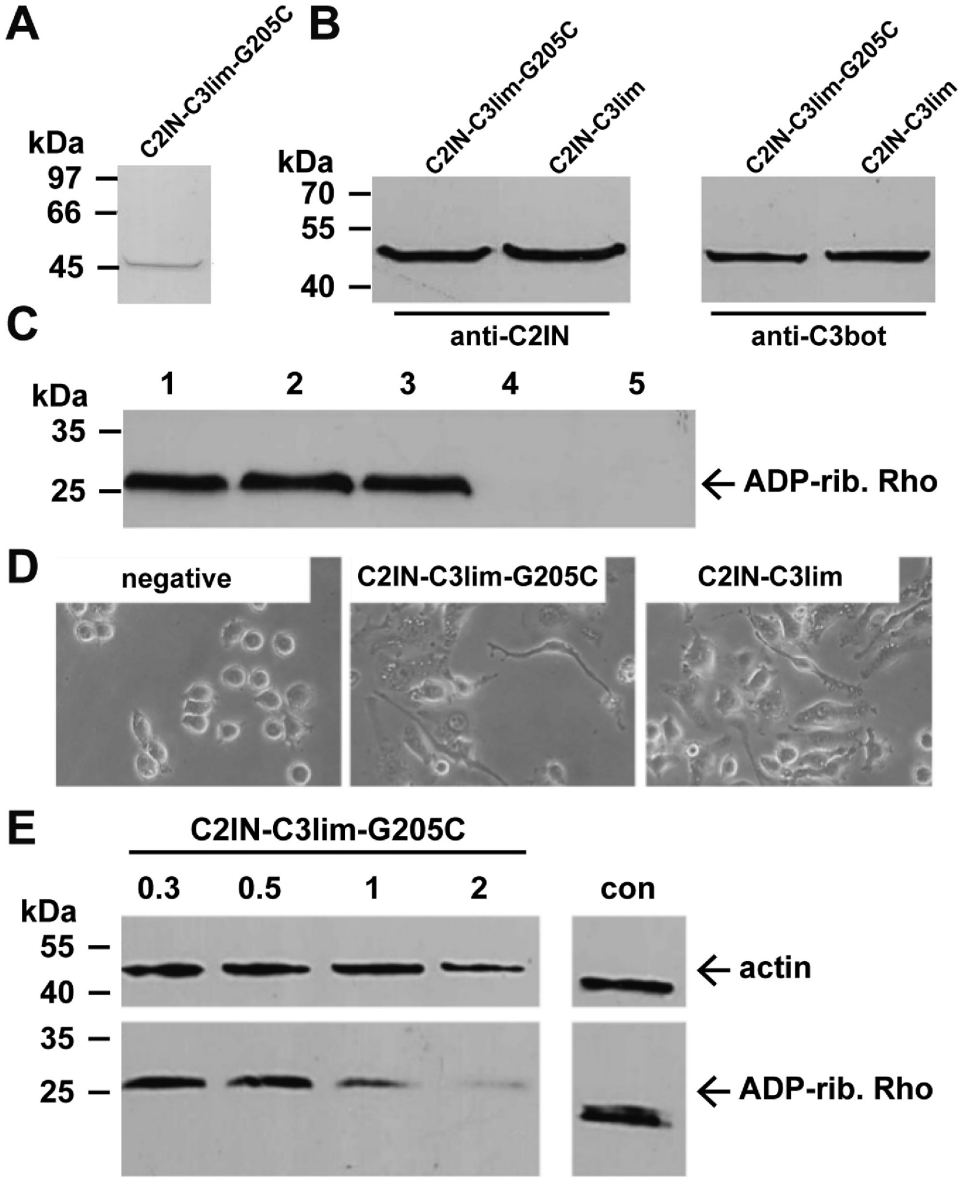

Figure 2. Characterization of C2IN-C3lim-G205C and the concentration-dependent ADP-ribosylation of Rho in living J774A.1 macrophages subsequent to the uptake of C2IN-C3lim-G205C. A) Coomassie blue staining of the expressed and purified fusion protein C2IN-C3lim-G205C after SDS-PAGE. B) SDS-PAGE of 400 ng C2IN-C3lim-G205C and 400 ng C2IN-C3lim for control followed by western blot. Complete expression of the fusion protein was confirmed by detecting protein moieties with specific antibodies against C2IN and C3. C) Lysate from CHO-K1 cells (40 µg) and the toxins C2IN-C3lim-G205C, C2IN-C3lim or C3lim (each 300 ng) were incubated in the presence of biotin-NAD$^+$ (10×10^{-6} M) for 30 min at 37 °C. As controls, cell lysate was either left untreated or was incubated only with biotin-NAD$^+$. Samples were separated by SDS-PAGE, blotted and biotinylated proteins were detected with streptavidin-peroxidase (1: 300 ng C2IN-C3lim-G205C, 2: 300 ng C2IN-C3lim, 3: 300 ng C3lim, 4: lysate with biotin-NAD$^+$, 5: lysate only). D) J774A.1 macrophages were treated for 8 h with either C2IN-C3lim-G205C (0.5 µg mL^{-1}), C2IN-C3lim (0.5 µg mL^{-1}) or were left untreated (negative). E) J774A.1 macrophages were concentration-dependent treated for 3 h with C2IN-C3lim-G205C (0.3, 0.5, 1, 2 µg mL^{-1}) or were left untreated as a control. Subsequently, cells were lysed and the lysates were incubated for 30 min at 37 °C with 300 ng C2IN-C3lim and 10×10^{-6} M biotin-NAD$^+$ to ADP-ribosylate Rho that was not ADP-ribosylated in the living cells. Subsequently, samples were subjected to SDS-PAGE and western blot and biotinylated proteins were then detected using streptavidin-peroxidase. Loading of comparable amounts of total protein was confirmed by actin staining with specific antibodies.

coupled to the DNA tag (Figures S1 and S2, Supporting Information). The results indicate that the treatment of the macrophages with the individual C2IN-C3lim fusion toxins did not kill the cells but rather altered their actin cytoskeleton via the C3-catalyzed ADP-ribosylation of Rho. Through the DNA tags, C2IN-C3lim-G205C could be readily loaded onto the DL2 linker under physiological conditions, thus the protein activity could be effectively maintained (data not shown). By mixing the C2IN-C3lim-G205C-loaded DL2 and PcP with a small amount of DL1 in water, the gelation occurred within 1 min at room temperature (RT). A temporally and spatially defined release of the intact C2IN-C3lim-G205C hydrogel cargo was achieved

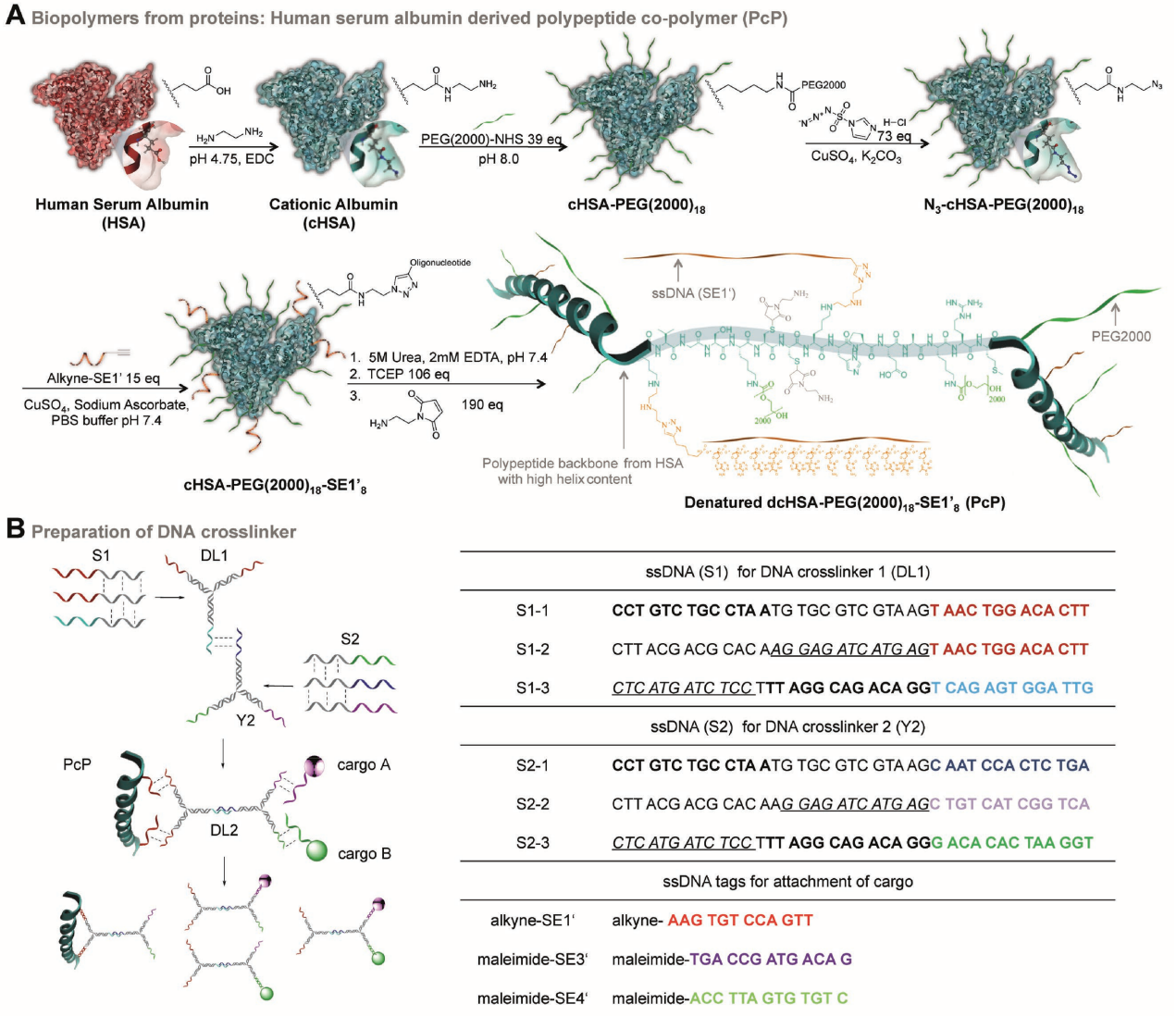

Figure 3. Scheme for the preparation of the hybrid protein–DNA hydrogel building blocks. A) Sequential preparation of human serum albumin (HSA)-derived polypeptide backbone (PcP) decorated with polyethylene glycol (PEG) and ssDNA (SE1′). B) Preparation of DNA crosslinker by DNA hybridization. Hybridizing sequences of the ssDNA as well as the respective sticky ends are indicated.

by enzyme-mediated degradation of the hydrogel by DNase I application.

2.3. Improved Hydrogel Stability by Chitosan

Because bone regeneration is a slow process, which necessitates controlled release of the toxin protein for several to tens of days, we have further developed a method to fine-tune and increase the stability of the hydrogel. A biocompatible cationic biopolymer – chitosan – was applied to interact with the negatively charged DNA linkers and to stabilize them through electrostatic interaction. Chitosan has been widely used for biocompatible hydrogel design and its biocompatibility has been frequently demonstrated.[32,33] We found that incubation of the hydrogel in chitosan solution (5 mg mL^{-1} in phosphate-buffered saline (PBS), pH 5 at 4 °C) for 2.5 h significantly prevented hydrogel degradation during cell experiments and prolonged the effective time of the hydrogel for slow protein release. The prepared hydrogels stabilized by chitosan treatment remained intact in PBS at 4 °C for 35 d. Moreover, the stabilized hydrogels remained intact in PBS at RT and 37 °C for several weeks, allowing for easy handling and administration. In contrast, the control hydrogel not incubated in chitosan degraded within 1 d when incubated at 4 °C in PBS (Figure S13, Supporting Information). Therefore, this observation indicates a highly increased stability of the hydrogel via noncovalent interactions. This could be advantageous for further in vivo application, allowing prolonged release of bioactive molecules from the hydrogels. These molecules might include anabolic factors, including growth factors, to stimulate bone formation, or antibiotics to fight periprosthetic infections, or

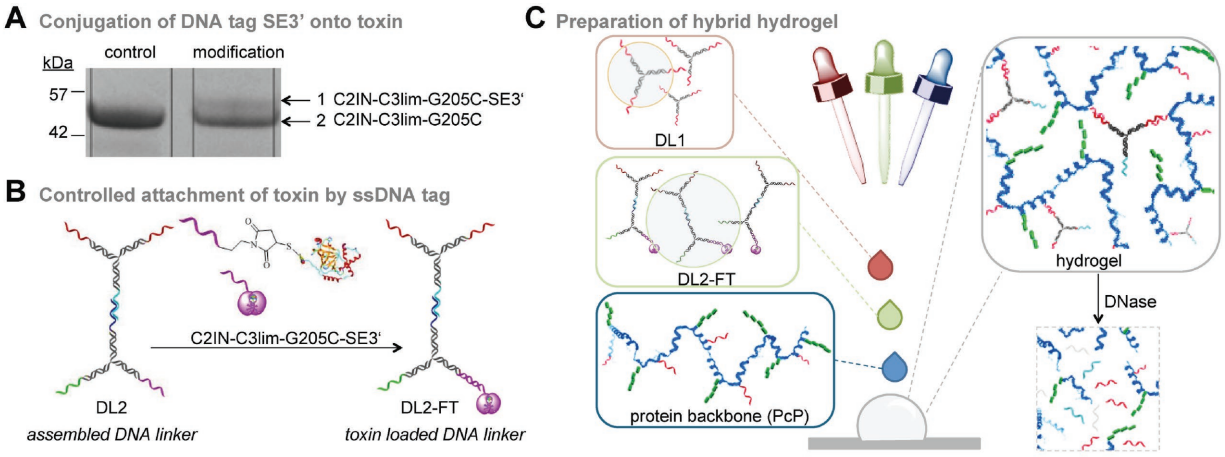

Figure 4. Scheme for the preparation of the toxin–DNA conjugate and the toxin-loaded hydrogel. A) Coomassie blue staining of the C2IN-C3lim-G205C-SE3′ DNA conjugate after SDS-PAGE. A total of 3 µg of the DNA conjugation reaction giving C2IN-C3lim-G205C-SE3′ and 3 µg C2IN-C3lim-G205C for control were subjected to SDS-PAGE. B) Preparation of the fusion toxin (FT) DNA conjugate DL2-FT by DNA-programed assembly. The ssDNA-modified C2IN-C3lim-G205C-SE3′ is used for DNA hybridization with DL2. C) Scheme for the preparation of C2IN-C3lim-G205C-loaded hydrogel with subsequent DNase-initiated degradation.

might target osteoclasts, thereby inhibiting bone resorption, for example, C3-toxin. Therefore, although hydrogels cannot be used for mechanical bone augmentation, in contrast to conventional cements, they may be useful for local drug release.

2.4. Mechanical Properties of the Stabilized Hybrid Hydrogel

To assess quantitatively the mechanical properties of the hybrid hydrogel, which are critical parameters for its function and applications, rheological characterization was performed. The oscillatory frequency sweep revealed typical viscoelastic behavior at lower frequencies, verifying the nature of a gel with the values of the storage modulus G' being higher than the corresponding values of the loss modulus G'' (**Figure 5**A). With increasing frequency, the loss modulus increased until intersection with the storage modulus occurred, indicating a phase transition from the gel to sol state at high frequencies. Moreover, mechanical stability over time was investigated by an oscillatory time-sweep test, measured at a fixed frequency (1 Hz) and strain (1%) (Figure 5B). The hydrogel exhibited constant mechanical strength with time, indicating that no structural rearrangements occurred within the hydrogel once gelation was completed. In addition, mechanical properties were investigated by an oscillatory strain sweep (0.01–1000%) at a fixed frequency (1 Hz) (Figure 5C). The values of G' and G'' remained constant in the low shear-stress region (<20%). However, with increasing oscillatory strain, G' decreased rapidly, whereas G'' increased slightly after the strain exceeded 40%. These results indicate the presence of a network structure, which does not collapse abruptly. However, microfissures within the network did form, which rapidly expanded to macrofractures, resulting in a gel-to-sol transition, indicating the collapse of the gel state to a quasi-liquid state at the intersection of G' and G'' at 123% strain. Moreover, the self-healing properties of the hydrogel were demonstrated by a combinatorial measurement, where the performed strain sweep was followed by an oscillatory time-sweep measurement at the same fixed frequency (1 Hz) used in the strain sweep and, importantly, a very low strain (0.1%) to avoid impacting structure formation during gel recovery (Figure 5D). This self-healing behavior of the hybrid hydrogel indicates that it could be applied in a straightforward fashion by simple injection directly to bone defects, thereby avoiding the need for surgical procedures to deliver the hydrogel into the body.

2.5. Inhibition of Osteoclast Formation and Bone Resorption by Hydrogel-Released C2IN-C3lim-G205C

To analyze C3-mediated toxicity in osteoclasts, hydrogel alone or hydrogel loaded with C3-derived recombinant fusion toxin C2IN-C3lim-G205C were incubated with RAW 264.7 cells in osteoclastogenic medium. The RAW 264.7 cell is a well-characterized preosteoclastic cell line, which is widely used as a model for osteoclast formation and activity.[34,35] Preliminary experiments showed that these cells were, like J774A.1 cells, susceptible to the cytotoxic effect of the recombinant fusion toxin (Figures S1 and S2, Supporting Information). Here, we investigated whether our hydrogel can serve as a potential carrier and controlled-release system for C2IN-C3lim-G205C to affect selectively bone cells in situ. The formation of multinucleated tartrate-resistant acid phosphatase (TRAP)-positive cells could be significantly reduced by 96% ($P < 0.001$ compared to control) after the treatment of RAW 264.7 cells with hydrogel loaded with C2IN-C3lim-G205C during the entire differentiation period, whereas cells incubated with hydrogel alone did not significantly differ from differentiated control cells (**Figure 6**A–E). Confirming these data, the resorption activity of RAW 264.7 cells after osteoclastogenic differentiation on a calcium phosphate-coated

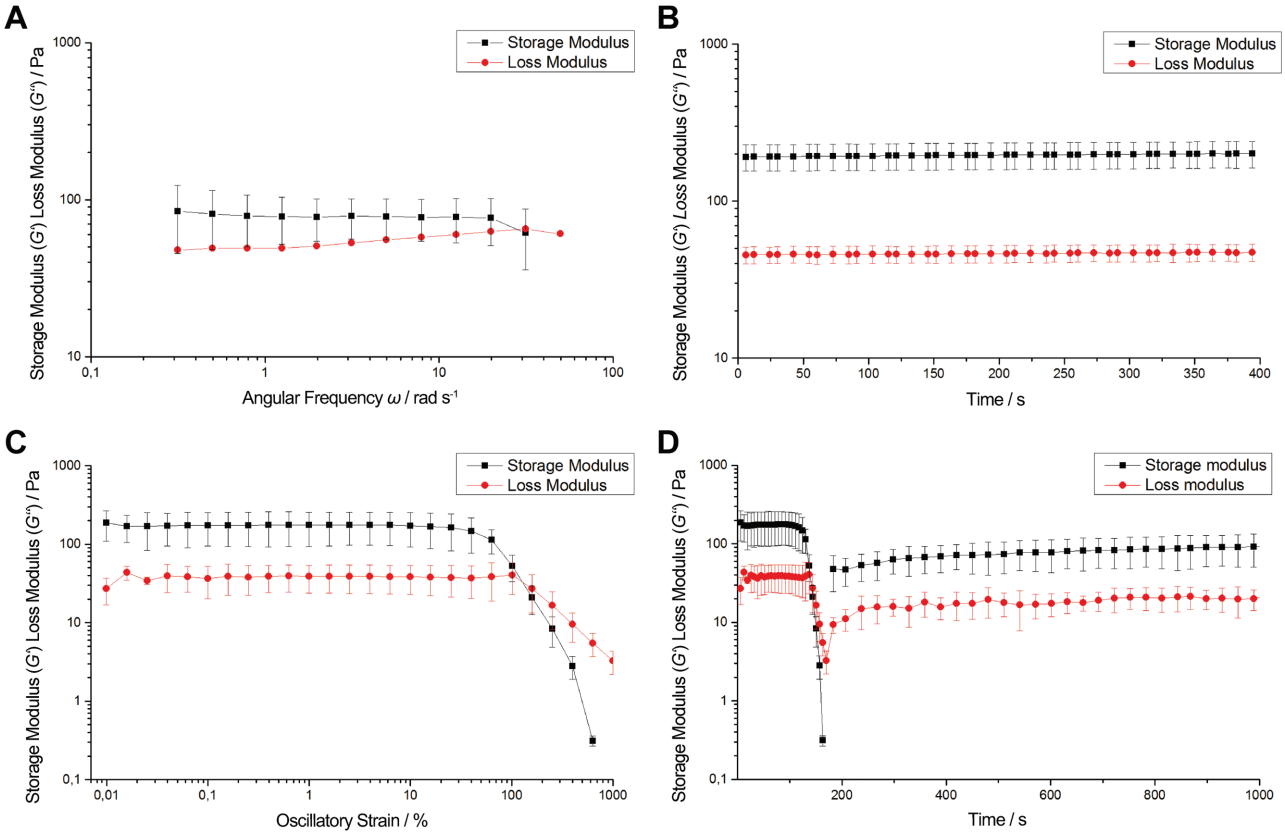

Figure 5. Rheological properties of chitosan-stabilized hybrid hydrogel. A) Frequency sweep (0.05–100 Hz) of 3.4% hydrogel at 25 °C with a fixed strain of 1%. Values are given as the mean ± standard deviation ($n = 2$). B) Oscillatory time sweep of 3.4% hydrogel for 5 min with a fixed strain of 1% and frequency of 1 Hz at 25 °C. Values are given as the mean ± standard deviation ($n = 3$). C) Oscillatory strain sweep (0.01–1000%) of 3.4% hydrogel at 25 °C with a fixed frequency of 1 Hz. Values are given as the mean ± standard deviation ($n = 2$). D) Oscillatory strain sweep (0.01–1000%) of 3.4% hydrogel at 25 °C with a fixed frequency of 1 Hz, followed by an oscillatory time sweep measurement with a fixed strain of 0.1% and frequency of 1 Hz at 25 °C. Values are given as the mean ± SD ($n = 2$).

surface with C2IN-C3lim-G205C-loaded hydrogel was significantly decreased, whereas hydrogels without toxin displayed no effect (Figure 6F–J). Therefore, in summary, hybrid hydrogels alone do not affect osteoclastogenic differentiation or the activity of osteoclast-like cells, whereas toxin-loaded hydrogels displayed a significant toxic effect, indicating effective C2IN-C3lim-G205C uptake into the cytosol. This corresponds to the described toxic effects when C2IN-C3lim was applied to macrophages, leading to the inhibition of Rho-mediated signaling, reorganization of the actin cytoskeleton, and a characteristic C3-mediated cell morphology.[26] Moreover, these data are in agreement with our previous findings, showing that C2IN-C3lim without a carrier could also affect morphology, viability, and osteoclastogenic differentiation of RAW 264.7 cells in a concentration-dependent manner more effectively than C3bot1.[25] Currently, the reason for the cell type-selective mode of action of C2IN-C3lim toward macrophage-like cells, including osteoclasts, remains unclear. However, one possible reason for the efficient internalization of C3 proteins into the cytosol of such cells may be that C3bot binds to proteinaceous structures on macrophages and that macrophages exhibit significantly more C3-binding sites compared to other cell types.[36]

2.6. Hydrogel-Released C2IN-C3lim-G205C Does Not Affect Osteoblast Viability or Differentiation

To confirm that the delivery of C2IN-C3lim-G205C toxin via hydrogel does not compromise osteoblast activity, osteoblast-like MC3T3-E1 cells were cultivated in osteogenic media with or without C2IN-C3lim-G205C immobilized in hybrid hydrogels. Cell proliferation and metabolic activity was evaluated by the MTT assay. No significant differences in cell viability were found between the groups (**Figure 7**A). Furthermore, analysis of the gene expression of the characteristic apoptosis marker tumor protein p53 and the proliferation marker KI67 showed, in agreement with the MTT analysis, no differences between the groups (Figure 7B,C). These results indicate that neither hydrogel alone nor C2IN-C3lim-G205C immobilized on hydrogel induced apoptosis or compromised cell proliferation. These data are in accordance with our previous studies showing that C2IN-C3lim cannot penetrate MC3T3-E1 cells without the separate transport component C2IIa, thereby not affecting Rho ADP-ribosylation in these cells.[25]

Osteogenic cell differentiation was analyzed by alkaline phosphatase staining and by the expression of osteogenic marker genes, including alkaline phosphatase (*Alpl*), osteocalcin

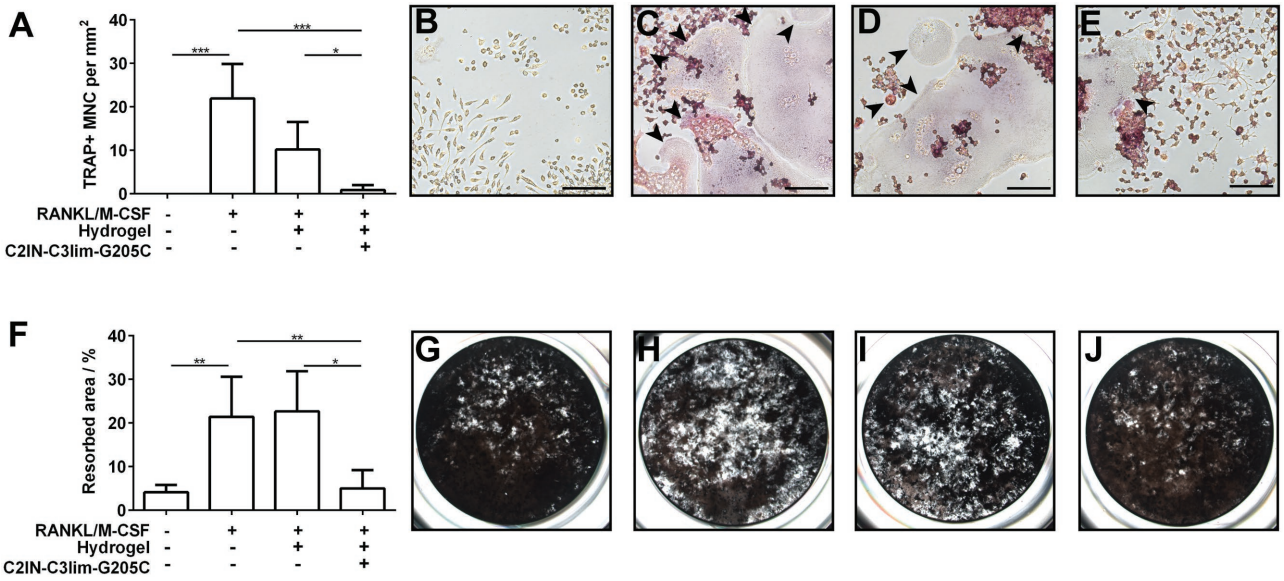

Figure 6. Effect of C2IN-C3lim-G205C released from protein–DNA hybrid hydrogel on the formation of mature osteoclast-like cells and their activity. Hydrogel comprising immobilized C2IN-C3lim-G205C (1 µg per 500 µL) was added to RAW 264.7 cells starting from day 1 and cells were treated with RANKL/M-CSF to induce osteoclast formation. Toxin release was enhanced by the addition of DNase I (50 or 100 U) to the hydrogel. A) The number of TRAP-positive multinucleated cells was determined after 5 d of incubation. B) Representative image of TRAP staining of untreated RAW 264.7 cells, C) cells after osteoclastogenic differentiation, and D) osteoclastogenic differentiation in the presence of unloaded hydrogel or E) C2IN-C3lim-G205C-loaded hybrid hydrogel. Scale bar is 100 µm. Arrowheads indicate TRAP-positive multinucleated cells. F) Quantification of resorbed area per well and G) representative von Kossa staining of a well with untreated RAW 264.7 cells, H) cells after osteoclastogenic differentiation, and I) osteoclastogenic differentiation in the presence of unloaded hydrogel or J) C2IN-C3lim-G205C-loaded hybrid hydrogel. Values are given as the mean ± SD (n = 12–15 for TRAP staining, n = 6–8 for pit assay), *=P < 0.05; **=P < 0.01; ***=P < 0.001.

(*Bglap*), and bone sialoprotein (*Ibsp*). We detected no significant differences in the alkaline phosphatase activity or gene expression between cells incubated in osteogenic differentiation medium with or without C2IN-C3lim-G205C-loaded hydrogels (Figure 7D–H), indicating that the hydrogel alone or the treatment with toxin did not compromise osteogenic differentiation of MC3T3-E1 cells. Osteocalcin gene expression was also significantly increased with both hydrogels. There was a nonsignificant increase in *Ibsp* expression in the presence of hydrogel. Therefore, our data clearly indicate that hybrid hydrogels either alone or loaded with C2IN-C3lim-G205C had no adverse or toxic effect on osteoblasts. In the osteoclast cell culture, C2IN-C3lim-G205C decreased osteoclast formation and activity, and these effects can be attributed to the toxin, because treatment with hydrogel alone did not affect the cells. However, the use of cell lines represents a limitation of the present study and implies the need for further evaluation using primary cells.

3. Conclusions

We have prepared a multifunctional hybrid hydrogel consisting of biodegradable and biocompatible components as well as a functional protein cargo as an efficient biomaterial for local treatment of bone diseases, including osteoporosis. The hybrid hydrogel is composed of chemically modified HSA and a rationally designed DNA linker. The hybrid hydrogel provides several advantageous features because of the mild and efficient DNA hybridization-based gelation, including: (1) rapid gelation under physiological conditions with crosslinking in the absence of chemically reactive, toxic groups or metal catalysts; (2) self-healing with favorable injectability allowing direct application to bone defects by simple injection,[14] (3) rapid, highly specific, and stable loading and controlled release of DNA-tagged cargo, ranging from proteins, enzymes, and growth factors to antibiotics. Considering all these properties, there are currently no other materials that provide a combination of all these features.

Recombinant C3 toxin (C2IN-C3lim-G205C) was effectively incorporated into the hybrid hydrogel, which fully maintained its bioactivity following bioconjugation. The spatiotemporally controlled C2IN-C3lim-G205C release allows efficient and specific inhibition of osteoclast formation and bone resorption, but does not affect osteoblastic differentiation and mineralization. The protein release by DNase application allows for local application of this hydrogel, which could provide inhibition of osteoclasts on a controlled time scale. This could provide not only a promising strategy to promote skeletal repair of bone diseases but also for local improvement of bone quality, for example, immediately surrounding bone implants. In addition, after releasing the therapeutic protein, this hydrogel is fully degradable and nontoxic, which is critical for noninvasive therapies.

In principle, because of the high functionalization capacity of the protein–DNA hybrid hydrogel, it is conceivable that it could stimulate bone formation by loading the hydrogel with anabolic factors, including growth factors, or to fight periprosthetic infections by loading it with antibiotics. In relation to this, instantaneous protein immobilization by simply adding the crosslinker immediately prior to injection or by applying moderate sheer forces would allow the application of very sensitive, less stable proteins. In this manner, the protein–DNA hybrid hydrogel

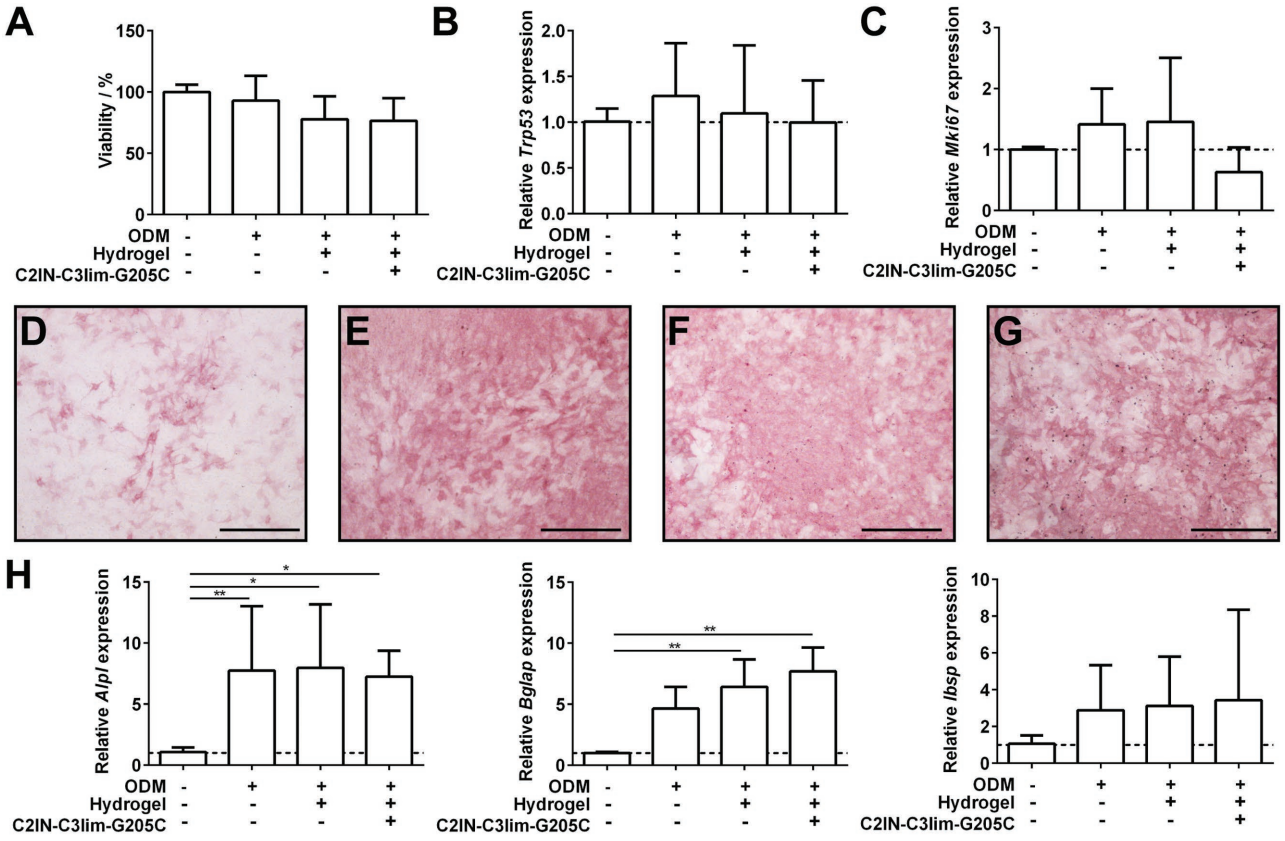

Figure 7. Effect of C2IN-C3lim-G205C delivered via hydrogel on osteoblast viability, proliferation, and differentiation. Hydrogel alone or hydrogel containing immobilized C2IN-C3lim-G205C (1 µg per 500 µL) was added to MC3T3-E1 cells cultivated with or without osteogenic differentiation medium (ODM). A) Cell viability as determined by the MTT assay. B) Expression of the apoptosis marker p53 and C) proliferation marker KI67. D) Representative alkaline phosphatase staining of MC3T3-E1 cell incubated without ODM, E) cells after osteogenic differentiation without and F) with hydrogel alone or G) with C2IN-C3lim-G205C-immobilized hybrid hydrogel. Scale bar is 500 µm. H) Relative expression of alkaline phosphatase (*Alpl*), osteocalcin (*Bglap*), and bone sialoprotein (*Ibsp*). Values are given as the mean ± SD (n = 15–22 for MTT assay, n = 6–10 for RT-qPCR analysis), *=P < 0.05; **=P < 0.01.

has great potential for the local improvement of bone quality in osteoporotic bone, for example, surrounding implants.[37–39] Moreover, using this strategy, patient-specific prophylactic treatment of bones with a high fracture risk, including vertebrae and the femoral neck, is also conceivable.[40–42]

4. Experimental Section

Materials and Instruments: HSA (>98%), bovine pancreatic deoxyribonuclease I (DNase I, lyophilized powder, protein ≥85%, ≥400 Kunitz units mg^{-1} protein), high-purity chitosan (M_v 40 000–60 000), DMT-dA(bz)-CPG, DMT-dT-CPG, DMT-dG(ib)-CPG, 1-ethyl-3-(3-dimethylaminopropyl) carbodiimide, ethylene diamine, and 5-hexyn-1-ol were obtained from Sigma-Aldrich Chemie GmbH (Munich, Germany). DMT-dA(bz) phosphoramidite, DMT-dT phosphoramidite, DMT-dG(iBu) phosphoramidite, and DMT-dC(Bz) phosphoramidite were obtained from Wuhu Huaren Science and Technology Co. (Wuhu City, Anhui Province, China). α-Methoxy-ω-carboxylic acid succinimidyl ester poly(ethylene glycol) was purchased from Iris Biotech GmbH (Marktredwitz, Germany). TCEP hydrochloride, urea, and ethylenediaminetetraacetic acid were obtained from Alfa Aesar (Karlsruhe, Germany). N-ethyldiisopropylamine was purchased from Merck Millipore (Darmstadt, Germany). 2-Cyanoethyl *N*,*N*-diisopropylchloro phosphoramidite was obtained from ChemGenes Corporation. TEAA 2.0 M buffer (pH 7) for high-performance liquid chromatography (HPLC) purification of DNA was purchased from Biosolve BV (Valkenswaard, Netherlands). Anti-C2IN and anti-C3 antisera were raised in rabbits (Pineda, Berlin, Germany). Horseradish-peroxidase-conjugated anti-rabbit and anti-mouse antibodies were obtained from Santa Cruz (Santa Cruz, Dallas, USA) and monoclonal anti-actin antibody from Sigma (Taufkirchen, Germany).

DNA synthesis was performed on a PolyGen 12-Column solid-phase DNA synthesizer (PolyGen GmbH). Purification of the synthesized DNA was accomplished by HPLC (1260 Infinity Quarternary LC System, Agilent Technologies) with a C18 RP-HPLC column (Agilent Eclipse XDB-C18, 5 µm, 9.4 × 250 mm, Agilent Technologies). The DNA concentration was determined using a NanoDrop 2000c from Thermo Fisher Scientific Inc. ÄKTA Purifier FPLC and a HighPrep_16/60 Sephacryl 300 HR column (GE healthcare, Munich, Germany) were used for polypeptide copolymer purification. A Superdex 200 Increase 10/300 GL column from GE healthcare was utilized for DNA linker purification. Agarose gel electrophoresis was conducted using the Bio-Rad Mini-Sub Cell GT horizontal electrophoresis system (Bio-Rad Laboratories GmbH). Sodium dodecyl sulfate (SDS) gel electrophoresis was performed using the Bio-Rad Mini-PROTEAN Tetra Cell electrophoresis system. Matrix-assisted laser desorption/ionization time-of-flight mass specta (MALDI-ToF MS) were recorded on a Bruker Reflex III MALDI-ToF MS spectrometer (Bruker Corporation). Rheological measurements were conducted on a DHR3 rheometer (TA Instruments). Characterization of chemical compounds by nuclear magnetic resonance spectroscopy

was conducted using a Bruker DRX 400 (^{1}H-NMR 400 MHz, ^{13}C-NMR 100 MHz, ^{31}P-NMR 162 MHz).

Vector Construction for the C3 Mutant – C2IN-C3lim-G205C: To create the cysteine-mutant of the fusion toxin C2IN-C3lim, glycine-205 was replaced by cysteine. The vector for the cysteine-C2IN-C3lim mutant was generated by site-directed mutagenesis with pGEX2T-C2IN-C3lim[30] as a template and the respective oligonucleotides using the Quick Change II XL site-directed mutagenesis kit (Agilent Technologies) according to manufacturer's instructions. One of the two complementary synthetic oligonucleotides is depicted here; C2IN-C3lim-G205C: 5′-CCTGAGTCAGCTATTATAACTACTATAA-AGTGCAAAGACTATATATTA-ATAGAAGGAAG-3′. The mutated plasmid was transformed into *E. coli* BL21 competent cells and the presence of the mutation confirmed by DNA sequencing.

Expression and Purification of the Recombinant C2IN-C3lim-G205C Mutant: C2IN-C3lim-G205C protein was expressed as a recombinant GST-fusion protein in *E. coli* as described earlier,[30] containing the respective DNA plasmid (C2IN-C3lim-G205C gene). Protein expression and enzymatic activity of the fusion protein was confirmed by SDS-PAGE and western blotting.

Macrophage Intoxication Assay to Evaluate Toxin Activity: J774A.1 macrophage-like cells (obtained from Dr. Singh Chhatwal, Braunschweig, Germany) were cultivated at 37 °C and 5% CO_2 in Dulbecco's modified Eagle medium (DMEM), containing 10% heat-inactivated (30 min at 56 °C) fetal calf serum (FCS). The medium contained L-glutamate (4×10^{-3} M), penicillin (100 U mL^{-1}), and streptomycin (100 mg mL^{-1}). Cells were reseeded at least twice weekly. For the intoxication assay, the cells were seeded in 12-well plates at a density of 125 000 cells per well in 1 mL medium. Afterward, the cells were incubated with toxin solutions: Either C2IN-C3lim-G205C (0.5 µg mL^{-1}) or C2IN-C3lim (0.5 µg mL^{-1}), which were added into the cell culture medium, or the cells were left untreated (negative control). At indicated time points, pictures were taken using a Zeiss Axiovert 40CFl microscope (Oberkochen, Germany) connected to a progress C10 CCD camera from Jenoptik (Jena, Germany). To detect in vitro enzyme activity of the new fusion-protein C2IN-C3lim-G205C, 40 µg of Chinese Hamster Ovary (CHO) cell lysate, including protease inhibitor, were incubated for 30 min at 37 °C in the presence of biotin-labeled NAD^{+} as cosubstrate for ADP-ribosylation and with 300 ng of C2IN-C3lim-G205C, C2IN-C3lim, or C3lim. The samples were denatured at 95 °C for 10 min and subjected to SDS-PAGE followed by western-blot analysis. Biotin-labeled ADP-ribosylated Rho was detected using a streptavidin-peroxidase system (MILLIPORE Immobilon Western, Billerica, USA) according to the manufacturer's instructions. Loading of comparable amounts of blotted protein was confirmed by detection of actin in the same blots.

MTS Assay: A total of 5000 RAW 264.7 cells or 8000 J774A.1 cells per well were seeded in 96-well plates overnight at 37 °C and 5% CO_2. Subsequently, the cells were incubated for 24, 48, and 72 h in a total volume of 100 µL containing either medium alone as control or C2IN-C3lim, C2IN-C3lim-G205C, or C2IN-C3lim-G205C-SE3′ at a final concentration of 2 or 1 µg mL^{-1}. Each sample was tested as a three-well replicate. The number of viable cells after incubation was determined using the CellTiter 96 AQ$_{ueous}$ One Solution Cell Proliferation Assay (MTS assay, Promega GmbH, Mannheim, Germany) according to the manufacturer's instructions.

Conjugation of Maleimide DNA to C2IN-C3lim-G205C Toxin – C2IN-C3lim-G205C-SE3′: Maleimide SE3′ (5.28 µL of 500 ng µL^{-1} stock solution in water, 663 pmol), C2IN-C3lim-G205C toxin (69.95 µL of 474 ng µL^{-1} solution in water, 663 pmol), and TCEP (12.02 µL, 5 ng µL^{-1}, 324 pmol, 0.3 eq) were mixed in PBS buffer (total volume of 100 µL) and incubated under gentle shaking for 4 h at RT. A conjugation yield of 30% was confirmed by SDS gel electrophoresis (10% gel, 2-(*N*-morpholino) ethanesulfonic acid buffer, 150 V, 50 min) and the modified toxin was stored at –20 °C until further use.

Preparation of Toxin-Loaded DNA Linker DL2-Fusion Toxin (FT) – DNA-Programed Assembly of C2IN-C3lim-G205C-SE3′ and DL2 DNA Linker: C2IN-C3lim-G205C-SE3′ (30 µg, 603 pmol) and DL2 (25.5 µg, 354 pmol) were mixed in PBS (26.55 µL total volume) and incubated under gentle shaking overnight at 4 °C to obtain the toxin-loaded DL2 linker (DL2-FT).

Preparation of Hybrid Hydrogel Comprising C2IN-C3lim-G205C: A total of 10 µL hydrogel comprising C2IN-C3lim-G205C toxin was prepared by mixing 2.25 µL PcP (15 wt%), 4.5 µL water (nuclease free), and 1.5 µL DL2-FT to obtain a final concentration of toxin in cell culture medium of 1 µg per 500 µL. Addition of 2.25 µL DL1 (2×10^{-3} M) resulted in hydrogel formation within seconds. To prepare 5 µL hydrogel, 1.13 µL PcP (15 wt%) was mixed with 2.3 µL water (nuclease free) and 0.45 µL DL2-FT to obtain a final concentration of the toxin in cell culture medium of 1 µg per 500 µL, followed by the addition of 1.13 µL DL1 (2×10^{-3} M) and rapid mixing of the components. Hydrogel formation occurred within few seconds.

Stabilization of Hybrid Hydrogel: Stabilization of the hydrogel was achieved by incubation in saturated chitosan solution (5 mg mL^{-1}, pH 5, 500 µL for 10 µL hydrogel and 150 µL for 5 µL hydrogel) for 2.5 h at 4 °C for cell experiments and rheological characterization or 3 h to determine stability.

Rheological Characterization: Rheological characterization was conducted using a DHR3 rheometer (TA Instruments) equipped with a temperature controller and a solvent reservoir to prevent hydrogel drying. Experiments were performed using an 8 mm parallel-plate geometry with 20 µL toxin-free hydrogels (DL2-FT was substituted by nuclease-free water) resulting in a gap size of 0.35 mm. In total, three different experiments were performed: (i) The linear viscoelastic region was found to be in the range of 1% strain and 1 Hz frequency. Therefore, oscillatory time-sweep measurements were performed at a fixed strain of 1% and a fixed frequency of 1 Hz at 25 °C for 5 min. (ii) Oscillatory strain sweeps (0.01–1000%) were conducted at a fixed frequency of 1 Hz at 25 °C. (iii) Frequency sweeps (0.05–100 Hz) were performed at a fixed strain of 1% at 25 °C.

Osteoclast Cell Culture: Murine monocytic RAW 264.7 cells (from LGC Standards GmbH/American Type Culture Collection (ATCC), Wesel, Germany) were incubated in DMEM (ATCC, Manassas, VA, USA) containing 10% FCS (Gibco, Darmstadt, Germany), 1% L-glutamine (Gibco), and 1% penicillin–streptomycin (Biochrom AG, Berlin, Germany) at 37 °C under a humidified atmosphere with 5% CO_2. To support the differentiation of RAW 264.7 cells into osteoclasts in vitro, the medium was supplemented with 20 ng mL^{-1} of murine recombinant receptor activator of nuclear factor-κB ligand (RANKL) and 10 ng mL^{-1} macrophage colony-stimulating factor (M-CSF).

Osteoclast formation was assessed by TRAP staining, seeding 2000 cells per well into 24-well plates. Resorption activity was evaluated by the pit assay, seeding 500 RAW 264.7 cells on calcium phosphate-coated 96-well plates. Coating was performed using SaOS2 cells as described in Lutter et al.[43] After 24 h, cell-culture medium was replaced with osteoclastogenic medium containing RANKL and M-CSF, and 10 µL hydrogel per 0.5 mL medium (24-well plates) or 5 µL hydrogel per 0.15 µL medium (96-well plates) was added. To avoid direct hydrogel/cell contact, the hydrogels were added into cell culture inserts placed into the wells. To enhance cargo release from the hydrogel, 100 U (10 µL hydrogel) or 50 U (5 µL hydrogel) DNase I was applied onto the hydrogel. After 5 d, TRAP staining was performed using a TRAP staining kit (Sigma) according to manufacturer's recommendations to analyze osteoclast formation. TRAP-positive cells with more than three nuclei were counted as osteoclasts (n = 12–15). To quantify TRAP staining, the mean number of TRAP^{+} multinucleated cells was calculated for each well by analyzing six visual fields per well under 100× magnification. Von Kossa staining was used to determine the resorption area using the image processing software Photoshop 6 (Adobe Systems) (n = 6–8). Here, the entire well area was set as the region of interest (ROI) and the threshold was set to the lightest (resorbed) area in the ROI. The percentage of resorbed area was calculated as the ratio of pixels after thresholding to the total number of pixels per ROI. All data were analyzed using Kruskal–Wallis with Dunn's post hoc test.

Osteoblast Cell Culture: Murine preosteoblastic MC3T3-E1 cell line (German Collection of Microorganisms and Cell Cultures, Braunschweig, Germany) was incubated in alpha-minimal essential medium (Gibco)

Table 1. RT-qPCR primer sequences.

Gene	Forward sequence	Reverse sequence
Gapdh	AACTTTGGCATTGTGGAAGG	CACATTGGGGGTAGGAACAC
Alpl	GCAGAGGTGATTGGCTTCT	GAGCCAGACCAAAGATGGAG
Bglap	GCGCTCTGTCTCTCTGACCT	ACCTTATTGCCCTCCTGCTT
Ibsp	GAAGCAGGTGCAGAAGGAAC	GAAACCCGTTCAGAAGGACA
Trp53	GGAAATTTGTATCCCGAGTATCTG	GTCTTCCAGTGTGATGATGGTAA
Mki67	GACAGCTTCCAAAGCTCACC	GTGTCCTTAGCTGCCTCCTG

supplemented with 10% FCS (PAA Laboratories, Pasching, Austria), 1% penicillin/streptomycin (Gibco), and 1% L-glutamine (Biochrom) at 37 °C under a humidified atmosphere with 5% CO_2. To induce osteogenic differentiation, the medium was additionally supplemented with 10×10^{-3} M β-glycerophosphate and 0.2×10^{-3} M ascorbate-2-phosphate (both Sigma-Aldrich; further denoted as osteogenic differentiation medium, ODM). A total of 20 000 cells were seeded per well in 24-well plates. After 24 h, the expansion medium was replaced with ODM containing 10 µL hydrogel per 0.5 mL medium. To avoid direct hydrogel/cell contact, the hydrogels were added into cell culture inserts placed into wells. Cargo release was enhanced from the hydrogel by the application of 100 U DNase I onto the hydrogel. Cell proliferation and metabolic activity were assessed after 7 d of osteogenic differentiation by the MTT assay as described previously.[25] Alkaline phosphatase protein expression was analyzed using the alkaline phosphatase staining kit (Sigma). Additionally, the expression of osteodifferentiation markers (alkaline phosphatase, osteocalcin, and bone sialoprotein), apoptosis marker p53, and proliferation marker KI67 were analyzed by real time quantitative PCR (RT-qPCR, n = 6–10). All data were analyzed using Kruskal–Wallis with Dunn's post hoc test.

Total RNA of samples was isolated using the Micro RNEasy Kit (Qiagen, Hilden, Germany) according to the manufacturer's protocol. A total of 1 µg of isolated RNA was subscribed into cDNA using the Omniscript Reverse Transcriptase Kit (Qiagen). Real-time PCR was performed using the Brilliant Sybr Green qPCR Master Mix Kit (Stratagene, Agilent Technologies, Munich, Germany) according to the manufacturer's instructions in a total volume of 25 µL as previously described.[44] Primer sequences are summarized in **Table 1**. Gene expression was normalized to the housekeeping protein glyceraldehyde 3-phosphate dehydrogenase (GAPDH).

Statistical Analysis: All results are presented as a mean ± standard deviation (SD). For experiments with RAW 264.7 and MC3T3-E1 cells, statistics software GraphPad Prism 6 (GraphPad Software, La Jolla, CA, USA) was used to evaluate the data, applying Kruskal–Wallis with Dunn's post hoc test. The level of significance was set to $P < 0.05$. All data were obtained from at least three independent experiments. Here, sample size was as follows: TRAP staining (n = 12–15), pit assay (n = 6–8), MTT assay (n = 15–22), real-time quantitative PCR (n = 6–10).

Supporting Information

Supporting Information is available from the Wiley Online Library or from the author.

Acknowledgements

J.G. and A.K. contributed equally to this work. The authors are grateful for the excellent support in the synthesis of several intermediates of the hydrogels to Nora Hartner, Dr. Matthias Arzt, and Magdalene Zimmermann and for the help with cell-culture experiments to Iris Baum. The study was funded by the Baden-Württemberg Stiftung (BioMatS-15), by the Horizon 2020 project "AD GUT" (No. 686271), and by the German Research Foundation (DFG) in the framework of the Collaborative Research Center CRC1149 (INST 40/491-1, INST 40/482-1) as well as the National Natural Science Foundation of China (No. 21534007).

Conflict of Interest

The authors declare no conflict of interest.

Keywords

clostridial Rho-inhibiting C3 toxin, hydrogels, osteoblasts, osteoclasts

Received: March 27, 2017
Revised: July 10, 2017
Published online: July 31, 2017

[1] J. A. Buza 3rd, T. Einhorn, *Clin. Cases Miner. Bone Metab.* **2016**, *13*, 101.
[2] R. Pacifici, *Ann. N. Y. Acad. Sci.* **2016**, *1364*, 11.
[3] N. A. Sims, *Int. J. Biochem. Cell Biol.* **2016**, *79*, 14.
[4] T. A. Asafo-Adjei, A. J. Chen, A. Najarzadeh, D. A. Puleo, *Curr. Osteoporosis Rep.* **2016**, *14*, 226.
[5] R. Dimitriou, E. Jones, D. McGonagle, P. V. Giannoudis, *BMC Med.* **2011**, *9*, 66.
[6] T. W. Axelrad, T. A. Einhorn, *Cytokine Growth Factor Rev.* **2009**, *20*, 481.
[7] L. Kyllonen, M. D'Este, M. Alini, D. Eglin, *Acta Biomater.* **2015**, *11*, 412.
[8] P. D. Miller, *Best Pract. Res., Clin. Endocrinol. Metab.* **2008**, *22*, 849.
[9] S. E. Papapoulos, *Best Pract. Res., Clin. Endocrinol. Metab.* **2008**, *22*, 831.
[10] N. A. Peppas, J. Z. Hilt, A. Khademhosseini, R. Langer, *Adv. Mater.* **2006**, *18*, 1345.
[11] J. A. Burdick, M. N. Mason, A. D. Hinman, K. Thorne, K. S. Anseth, *J. Controlled Release* **2002**, *83*, 53.
[12] T. Ito, M. Saito, T. Uchino, M. Senna, M. Iafisco, M. Prat, L. Rimondini, M. Otsuka, *J. Mater. Sci.: Mater. Med.* **2012**, *23*, 1291.
[13] Y. Gao, S. Zhu, E. Luo, J. Li, G. Feng, J. Hu, *J. Controlled Release* **2009**, *139*, 15.
[14] Y. Wu, C. Li, F. Boldt, Y. Wang, S. L. Kuan, T. T. Tran, V. Mikhalevich, C. Fortsch, H. Barth, Z. Yang, D. Liu, T. Weil, *Chem. Commun.* **2014**, *50*, 14620.
[15] C. S. Hughes, L. M. Postovit, G. A. Lajoie, *Proteomics* **2010**, *10*, 1886.
[16] Y. Wu, G. Pramanik, K. Eisele, T. Weil, *Biomacromolecules* **2012**, *13*, 1890.
[17] Y. Wu, K. Eisele, M. Doroshenko, G. Algara-Siller, U. Kaiser, K. Koynov, T. Weil, *Small* **2012**, *8*, 3465.
[18] Y. Wu, S. Ihme, M. Feuring-Buske, S. L. Kuan, K. Eisele, M. Lamla, Y. Wang, C. Buske, T. Weil, *Adv. Healthcare Mater.* **2013**, *2*, 884.
[19] D. Y. Ng, Y. Wu, S. L. Kuan, T. Weil, *Acc. Chem. Res.* **2014**, *47*, 3471.
[20] Y. Wu, S. Chakrabortty, R. A. Gropeanu, J. Wilhelmi, Y. Xu, K. S. Er, S. L. Kuan, K. Koynov, Y. Chan, T. Weil, *J. Am. Chem. Soc.* **2010**, *132*, 5012.
[21] S. Alcazar-Leyva, E. Ceron, F. Masso, L. F. Montano, P. Gorocica, N. Alvarado-Vasquez, *Med. Sci. Monit.* **2009**, *15*, CR51.
[22] H. J. Fuchs, D. S. Borowitz, D. H. Christiansen, E. M. Morris, M. L. Nash, B. W. Ramsey, B. J. Rosenstein, A. L. Smith, M. E. Wohl, *N. Engl. J. Med.* **1994**, *331*, 637.

[23] J. C. Davis Jr., S. Manzi, C. Yarboro, J. Rairie, I. McInnes, D. Averthelyi, D. Sinicropi, V. G. Hale, J. Balow, H. Austin, D. T. Boumpas, J. H. Klippel, *Lupus* **1999**, *8*, 68.
[24] A. J. Johnson, P. R. Goger, W. S. Tillett, *J. Clin. Invest.* **1954**, *33*, 1670.
[25] A. Tautzenberger, C. Fortsch, C. Zwerger, L. Dmochewitz, L. Kreja, A. Ignatius, H. Barth, *PLoS One* **2013**, *8*, e85695.
[26] J. Fahrer, J. Kuban, K. Heine, G. Rupps, E. Kaiser, E. Felder, R. Benz, H. Barth, *Cell. Microbiol.* **2010**, *12*, 233.
[27] M. Vogelsgesang, A. Pautsch, K. Aktories, *Naunyn-Schmiedeberg's Arch. Pharmacol.* **2007**, *374*, 347.
[28] K. Aktories, J. Frevert, *Biochem. J.* **1987**, *247*, 363.
[29] I. Just, C. Mohr, G. Schallehn, L. Menard, J. R. Didsbury, J. Vandekerckhove, J. van Damme, K. Aktories, *J. Biol. Chem.* **1992**, *267*, 10274.
[30] H. Barth, F. Hofmann, C. Olenik, I. Just, K. Aktories, *Infect. Immun.* **1998**, *66*, 1364.
[31] K. Eisele, R. A. Gropeanu, C. M. Zehendner, A. Rouhanipour, A. Ramanathan, G. Mihov, K. Koynov, C. R. W. Kuhlmann, S. Vasudevan, H. J. Luhmann, T. Weil, *Biomaterials* **2010**, *31*, 8789.
[32] N. Bhattarai, J. Gunn, M. Zhang, *Adv. Drug Delivery Rev.* **2010**, *62*, 83.
[33] J. K. Suh, H. W. Matthew, *Biomaterials* **2000**, *21*, 2589.
[34] S. A. Clarke, J. Martin, J. Nelson, J. C. Hornez, M. Bohner, N. Dunne, F. Buchanan, *Adv. Healthcare Mater.* **2017**, *6*, 1600947.
[35] M. Maycas, M. T. Portoles, M. C. Matesanz, I. Buendia, J. Linares, M. J. Feito, D. Arcos, M. Vallet-Regi, L. I. Plotkin, P. Esbrit, A. R. Gortazar, *J. Cell. Physiol.* **2017**, DOI: 10.1002/jcp.25829.
[36] A. Rohrbeck, L. von Elsner, S. Hagemann, I. Just, *Naunyn-Schmiedeberg's Arch. Pharmacol.* **2014**, *387*, 523.
[37] J. Karlsson, A. Martinelli, H. M. Fathali, J. Bielecki, M. Andersson, *J. Biomed. Mater. Res., Part A* **2015**, *104*, 620.
[38] U. Kettenberger, V. Luginbuehl, P. Procter, D. P. Pioletti, *J. Tissue Eng. Regener. Med.* **2015**, *11*, 1974.
[39] D. Oliveira, J. S. Hassumi, P. H. Gomes-Ferreira, T. O. Polo, G. R. Ferreira, L. P. Faverani, R. Okamoto, *J. Appl. Oral Sci.* **2017**, *25*, 42.
[40] R. Aquarius, J. Homminga, A. J. Hosman, N. Verdonschot, E. Tanck, *Med. Eng. Phys.* **2014**, *36*, 944.
[41] C. K. Chiang, Y. H. Wang, C. Y. Yang, B. D. Yang, J. L. Wang, *Spine* **2009**, *34*, 356.
[42] L. Fliri, A. Sermon, D. Wahnert, W. Schmoelz, M. Blauth, M. Windolf, *J. Biomater. Appl.* **2013**, *28*, 136.
[43] A. H. Lutter, U. Hempel, C. Wolf-Brandstetter, A. I. Garbe, C. Goettsch, L. C. Hofbauer, R. Jessberger, P. Dieter, *J. Cell. Biochem.* **2010**, *109*, 1025.
[44] A. Liedert, D. Kaspar, L. Claes, A. Ignatius, *Biochem. Biophys. Res. Commun.* **2006**, *342*, 1070.